International Journal of Mechanical Engineering (IJME)
ISSN: 2319-2240
Vol.2, Issue 1 Feb 2013 29-36

International Academy of Science, Engineering and Technology
Connecting Researchers; Nurturing Innovations

EFFECT OF ANGLE OF FLAP ON LIFT AND DRAG IN A FLAPPING WING FLIGHT

B.BALAKRISHNA[1], P. SRI SESHAVANI[2] & P. RAVINDER REDDY[3]

[1]Associate Professor, Department of Mechanical Engineering, University College of Engineering, JNTU Kakinada, India

[2]PG Student, Department of Mechanical Engineering, University College of Engineering, JNTU Kakinada, India

[3]Professor and Head, Department of Mechanical Engineering**,** Chaitanya Bharathi Institute of Technology, Gandipet, Hyderabad, India

ABSTRACT

The aim of this work is to evaluate the influence of angle of flap on lift and drag in a flapping wing flight. To do so aerodynamic analysis is carried on flap wing using CFD simulations. Flapping wing aerodynamic performance has been only concentrated on motion under calm and clear atmospheric conditions. Small atmospheric disturbance such as gust wind could lead to flapping MAV (Micro Aerial Vehicle) great damage. FLUENT software was adopted for the motions of flapping wing. By considering unsteady flow of 3-D flapping wing, the aerodynamic parameters considered are lift and thrust. Finally, the flapping wing behavior is simulated in gust wind conditions through existing gust wind profile, and results shows that the lift did change with the wind speed. As wind speed becomes larger, the lifts also vary violently and lead to detrimental situations. Weather influence always observed for the design of wing.

KEYWORDS: Kinematic Parameters, Wing Rotation, Clap, Fling, Aerodynamic Characteristics

INTRODUCTION

Among flying animals only insects and hummingbirds are capable of sustained hovering. The reciprocation of their wings at high frequencies affords high maneuverability, rapid ascent, and carriage of loads greater than body mass, a feat that is routinely accomplished by many insects, such as during undertaking in honey bees, blood-feeding in mosquitoes and prey carriage in cicada-hunting wasps. Over a million different species of insects fly with flapping wings, and 10,000 types of birds and bats flap their wings for locomotion. This proliferation of flying species has also attracted scientific attention. Biologists and naturalists have produced kinematic descriptions of flapping wing motion and empirical correlations between flapping frequency, weight, wingspan, and power requirements based on studies of many different families of birds and insects. Bio-fluid dynamicists have attempted to explain the underlying physical phenomena both in the quasi-steady limit and in the fully unsteady regime. Kinematic parameters[1] such as wing beat frequency (n) and wing stroke amplitude (Φ) (Altshuler and Dudley, 2003; Dudley, 1995; Lehmann, 2004; Roberts et al., 2004) that contribute to the angular and translational velocity of the wing and lift produced via delayed stall (Dickinson et al., 1999; Sane, 2003; Sane and Dickinson, 2002). However, several other possible strategies exist for varying hovering flight forces, such as changing angle of attack, wing rotation velocity/timing, and 'clap and fling' (Sane, 2003).

A limited amount of work has been completed in regards to the development of dynamic models and control schemes to successfully operate a flapping wing micro-air vehicle. Sun and Wang [2] acknowledge that the field of aerodynamics, in regards to insect flight, is highly studied. The main purpose of reference [2] is to produce a quantitative analysis of the stability of hovering flight for a model insect. The authors chose a dynamics model previously given in [7, 8]. The dynamics model chosen is the standard, linearized aircraft dynamics that can be found in [9]. In contrast to the Taylor and Thomas model [8], Sun and Wang use stability and control derivatives calculated by CFD methods.

Conventional aerodynamic theories, owing to the intrinsic assumptions of quasi-steady flow incorporated in them, are inadequate to explain the superior aerodynamic performance of insect wings [10]. Flapping wings produce substantially higher aerodynamic forces than those predicted by quasi-steady theories. The failure of such theories, in turn, propelled the research in exploring the unsteady aerodynamic mechanisms employed by insects. Recent flow visualization studies on tethered and free-flying real insects [11–15], experiments performed using dynamically scaled-up models of flapping insect wings [16–22] and numerical simulations of idealized wing motions [23–29] have successfully revealed and provided deeper insights into some of the possible mechanisms used by insects during hovering and in some maneuvering flight. Smoke flow visualizations over a tethered hawkmoth, Manduca sexta and its similarity preserved flapping mechanical model identified an intense attached Leading Edge Vortex (LEV), of sufficient strength to explain the high-lift forces [12].

Dynamically scaled experiments on the model fruitfly wings demonstrated the aerodynamic benefits of wing rotation [16]. Rapid rotation of wings during stroke reversal acted as a source of additional circulation and enhanced the aerodynamic forces produced. The authors assessed that this mechanism was similar to Magnus effect, and was termed as rotational circulation. In order to understand how modifications in wing kinematics alter the aerodynamic forces generated by a moving wing and hence to understand how insects precisely alter the kinematics for different aerial maneuvers, Sane and Dickinson [18] studied 191 separate sets of kinematic patterns. Influences of the following behaviorally important kinematic parameters were studied: stroke amplitude, AOA, flip timing, flip duration, and the shape and magnitude of stroke deviation. The stroke velocity was varied as a trapezoidal function of time, which was the kinematics obtained from tethered fruitfly. Recently, Wu and Sun [26] computed the aerody-namic forces generated by a model fruitfly wing, in which translational velocity was varied as a simple harmonic function. The consequences of varying the following important kinematic parameters, through 2D numerical simulations, are examined in detail to understand the fluid dynamics of inclined stroke plane motions: Reynolds number (Re), stroke amplitude (A_0), rotational timing and rotational duration (Dsr). Although, it has been found that spanwise flow is important in stabilizing the vortex in high Re (≈5000) hawkmoth hovering [12, 23], studies on fruitfly flapping observed no evidence of spanwise flow [17] at low Re (_110) flow. Since the maximum Re considered in our simulations is 150, 2D study can be appropriate in capturing the LEV. Despite the difference in the LEV structures, the agreement between 3D dragonfly wings and 2D computation was quite good [27]. In a recent study [32], 2D numerical simulations were compared against 3D robotic wing experiments.

MODELING AND MESHING CFD ANALYSIS

The geometry of the wing and meshing was created in Gambit software and analysis is done in fluent software. Aerofoil geometry is NACA0014, since the airfoil geometry is defined by sets of coordinate points, the more points defined will increase the accuracy of the model. An airfoil geometry defined by one hundred points for both the top and bottom surface will result in a good definition. The list of coordinates were derived by scripting equations into a Mat lab M-file, which then supplied the corresponding x, y, and z coordinate for each of the hundred points along the upper and lower surface of the airfoil (Figure1). Meshing is made in Gambit and imported Fluent solver for analysis.

RESULTS AND DISCUSSIONS

After the completion of CFD simulations for studying the aerodynamic characteristics of flapping wing, the obtained results are shown in table1 and shows the variation of temperature, pressure and velocity with respect to position of the wing flap. It can observed from the obtained results are the maximum temperature of 313.^{0} k is obtained at -45^0,-30^0, -15^0, 30^0, 45^0 flapping position from there it gradually decreases until a minimum temperature of 312^0 k at -60^0, 0^0, 15^0, 60^0 flap position.

Table 1: The Variation of Temperature, Pressure and Velocity with Respect to Position of the Flap with Horizontal

Angle, Degrees	Temperature Variation, ^{0}k	Pressure Variation, Pa	Velocity Variation, m/s
-60	312	14800	405
-45	313	13700	413
-30	313	13000	414
-15	313	14200	417
0	312	14200	415
15	312	14700	408
30	313	15300	407
45	313	14000	411
60	312	12800	415

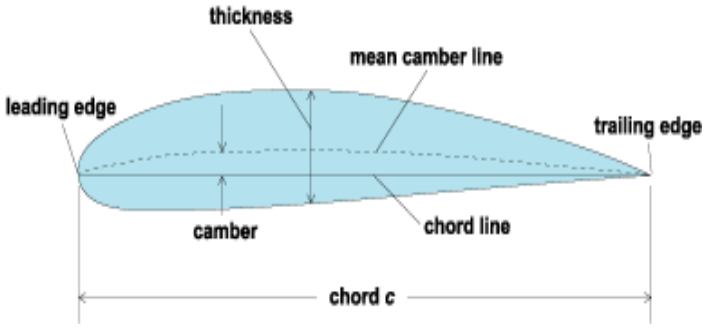

Fig. 1: Aerofoil

The temperature variation is seen due to the following reason, when air encounters a fast moving flapping wing the air near the leading edge is a most stopped and its kinetic energy is converted into heat energy. After the air gets deflected and flows over the aerofoil there is a variation in temperature because of the heated air flowing on the wing and there is a free stream of air above the hot air which exchanges heat with it and causing a temperature difference along the wing. It shows the variation of temperature, pressure and velocity with respect to position of the wing flap. It can be observed from the obtained results are the maximum pressure of 15300 pa is observed at 30^0 flapping position from there it gradually decreases until a minimum pressure of 14200 pa at 0^0 flap position and then gradually increases to 14700 pa at 15^0 flap position during the flapping flight.

The pressure variation is seen due to the following reason Bernoulli's principle of pressure by itself does not explain the distribution of pressure over the upper surface of the wing. It can be observed from the obtained results as shown in table.1 that the maximum velocity of 417 m/s is obtained at -15^0 flapping position and the next highest is seen at 15^0 flap angle of velocity 415 m/s then there a gradually decreases of velocity upto 405 m/s at -60^0 flap position and then increases to 413 at -45^0 flap position and from there it decreases to 407at 30^0 flap position. The maximum Mach number of 1.2 is obtained at 45^0 flapping position and the next highest is seen at -45^0 flap angle of Mach number of 1.21 then there is a decreases of Mach number up to 1.16 at -30^0 flap position and then increases to 1.18 at -15^0 flap position and from there it decreases to 1.13 at 30^0 flap position.

Table2 shows the variation of Mach number and turbulence variation with respect to position of the wing flap. The maximum Mach number of 1.2 is obtained at 45^0 flapping position and the next highest is seen at -45^0 flap angle of Mach number of 1.21 then there is a decreases of Mach number up to 1.16 at -30^0 flap position and then increases to 1.18 at -15^0 flap position and from there it decreases to 1.13 at 30^0 flap position.

Table 2: The Variation of Mach Number and Turbulence Variation with Respect to Position of the Flap with Horizontal

S.No.	Angle	Mach Number	Turbulence Variation	
	(Degrees)	(Dimension Less Number)	Modified Turbulent Viscosity	Turbulent Viscosity Ratio
			(m^2/s)	(dimensionless number)
1	-60	1.12	0.000184	10.01
2	-45	1.21	0.000194	10.09
3	-30	1.16	0.000182	9.89
4	-15	1.18	0.000184	10.01
5	0	1.22	0.000187	10.04
6	15	1.14	0.000184	10.01
7	30	1.13	0.000187	10.03
8	45	1.20	0.000187	8.98
9	60	1.16	0.000185	9.92

Since the speed of sound increases as the temperature increases, the actual speed of an object travelling at Mach 1 will depend on the fluid temperature around it. Mach number is useful because the fluid behaves in a similar way at the same Mach number. At transonic speeds, the flow field around the object includes both sub and supersonic parts. The transonic period begins when first zones of M>1 flow appear around the object. In case of an airfoil (such as an aircraft's wing), this typically happens above the wing. Supersonic flow can decelerate back to subsonic only in a normal shock, this typically happens before the trailing edge. As the speed increases, the zone of M>1 flow increases towards both leading and trailing edges. As M=1 is reached and passed the normal shock reaches the trailing edge and becomes a weak oblique shock, the flow decelerates over the shock, but remains supersonic. A normal shock is created ahead of the object, and the only subsonic zone in the flow field is a small area around the object's leading edge. Table 3 the co-efficient of lift with respect to position of the wing flap. That the maximum lift co-efficient of 8.60e4 is obtained at 0^0 flapping position and the next highest is seen at 15^0 flap angle of lift coefficient of 7.8e4 then there is gradual decreases of lift coeffient up to 6.00e4 at 45^0 flap position and the minimum is seen at -60^0 flap position of 4.00e4 increases to 8.6e4 at 0^0 flap position.

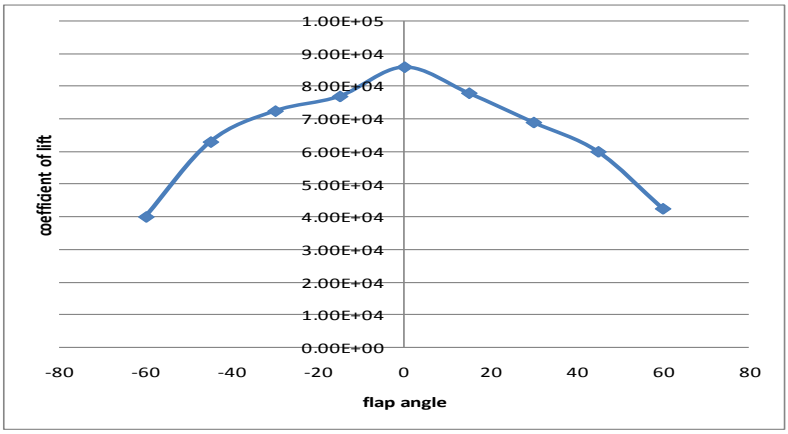

Fig. 2: Variation of Coefficient of Lift with Respect to Flap Angle

Lift coefficient may be used to relate the total lift generated by an aircraft to the total area of the wing of the aircraft. In this application it is called the aircraft or plan-form lift coefficient. The lift coefficient is given by

$$C_L = \frac{L}{\left(\frac{1}{2}\right)\rho v^2 A} = \frac{2L}{\rho v^2 A} = \frac{L}{qA} \quad (1)$$

Where L is the lift force, ρ is fluid density, υ is true air speed, q is the Dynamic pressure, A is the plan-form area and the lift coefficient is dimensionless number. As from the above formula we can see that lift is directly proportional to plan-form area and as the effective area decreases for higher angles of flap position so, the lift decreases for higher angles of flap position and for smaller flap positions the higher lift is observed. From the experimental data obtained we can observe that higher lift coefficient is obtained at smaller flap angles and lift coefficient decreases at higher flap angles. From the figure2, it is evident that at higher flap angles i.e . at -45^0, 45^0 the lift is very low and at least flap angles i.e., at -15^0, 0^0, $15^0$the lift is maximum, so we need to take care that the amplitude of the wing flapping sysytem should not be more than 60^0 in the total so that maximum lift can be achieved. The coefficient of drag with respect to position of the wing flap. It can be observed from the maximum drag coefficient of 6.25e4 is obtained at $\pm 60^0$ flapping position and the next highest is seen at -45^0 flap position angle of drag coefficient of 4.415e4 then there is a gradual decreases of drag coefficient upto 3.248e4 at -15^0 flap position and there is a rise in drag at 0^0 of 3.284e4 and at 15^0 flap position drag coefficient of 3.309e4 is observed and at 30^0 flap position drag coefficient of 3.264e4 is seen. In fluid dynamics, the drag coefficient is a dimensionless quantity that is used to quantify the drag or resistance of an object in a fluid environment such as air or water. The coefficient drag gives the amount of drag force generated as the angle of flap increases more amount of air flow is een at the lower end of the flapping wing so that drag force increases more higher flapping angles in a flapping flight. We have from the experimental results that the coefficient of drag is more for higher flapping angle (refer Fig.3) and decreases as the flapping angle decreases.

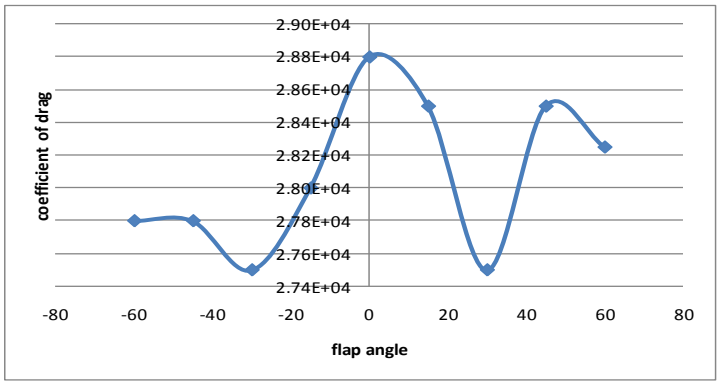

Fig. 3: Variation of Coefficient of Drag with Respect to Flap Angle

The coefficient of moment deals with the unbalancing forces acting on the wing. The unbalancing force is maximum at -45^0 having the value of 10.905e4. the graph between coefficient of moment and angle of flap is shown in figure 4.

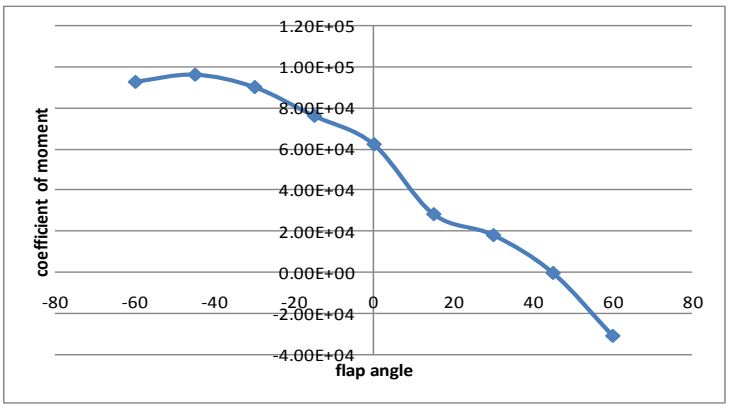

Fig. 4: The Coefficient of Moment with Respect to Position of the Flap with Horizontal

CONCLUSIONS

At high angles of attack, stall occurs and lift decreases drastically. At low angles of attack, there is an improvement in the aerodynamic characteristics of the wing. The flapping wing behaves differently at different angles of attack. At ± 60º flap angles of wing drag co-efficient is increased. At ± 60º flap angles of wing the temperature increases to ≈ 313 ^{0}K. At - 60º flapping angle of wing the co-efficient of moment is increasing 9.25e4. At ± 60º flapping angles of wing pressure is increasing to 12800 pa. At ± 60º flapping angles of wing velocity is increasing to 405 m/s. At ± 60º flapping angles of wing Mach number increases to 1.

REFERENCES

1. Jason Thomas Vance Experimental and natural variation in hovering flight capacity in bees, Hymenoptera: Apidae, University of Nevada Las Vegas
2. M. Sun and J.K. Wang. Flight stabilization control of a hovering model insect. The Journal of Experimental Biology, 210:2714–2722, 2007.
3. W. Shyy, Y. Lian, J. Tang, D. Viieru, and H. Liu. Aerodynamics of low Reynolds number flyers. Cambridge University Press, New York, NY, 2008.
4. W. Shyy, Y. Lian, J. Tang, H. Liu, P. Trizilia, B. Stanford, L. Bernal, C. Cesnik, P. Friedmann, and P. Ifju. Computational aerodynamics of low reynolds number, plunging, pitching and flexible wings for mav applications. Acta Mechanica Sin, 24:351–373, 2008.
5. H. Baruh. Analytical Dynamics. WCB McGraw-Hill, Boston, MA, 2006.
6. P. Trizilia, C. Kang, M. Visbal, and W. Shyy. Low reynolds number hovering wing aeroydynamics: performance, tip vortices, and induced jet. Submitted to Journal of Fluid Mechanics, 2009.
7. M. Sun and Y. Xiong. Dynamic flight stability of a hovering bumblebee. The Journal of Experimental Biology, 208:447–459, 2005.
8. G. Taylor and A. Thomas. Dynamic flight stability in the desert locus Schistocerca gregaria. The Journal of Experimental Biology, 206:2803–2829, 2003.
9. B. Etkin and L.D. Reid. Dynamics of flight. John Wiley and Sons, New York, NY, 1996.
10. Ellington CP. The aerodynamics of hovering insect flight. I. The quasi-steady analysis. Phil Trans R Soc Lond Ser B 1984;305:1.
11. Dickinson MH, Lehmann FO, Götz KG. The active control of wing rotation by Drosophila. J Exp Biol 1993;182:173.
12. Ellington CP, Van den Berg C, Willmont AP, Thomas ALR. Leading edge vortices in insect flight. Nature 1996;348:626.
13. Lehmann FO, Dickinson MH. The control of wing kinematics and flight forces in fruitflies (Drosophila spp.). J Exp Biol 1998;201:384.
14. Srygley RB, Thomas ALR. Unconventional lift-generating mechanisms in freeflying butterflies. Nature 2002;420:660.

15. Thomas ALR, Taylor GK, Srygley RB, Nudds RL, Bomphrey RJ. Dragonfly flight: free-flight and tethered flow visualizations reveal a diverse array of unsteady lift-generating mechanisms, controlled primarily via angle of attack. J Exp Biol 2004;207:4299.
16. Dickinson MH, Lehmann FO, Sane SP. Wing rotation and the aerodynamic basis of insect flight. Science 1999;284:1954.
17. Birch JM, Dickinson MH. Spanwise flow and the attachment of the leadingedge vortex on insect wings. Nature 2001;412:729.
18. Sane SP, Dickinson MH. The control of flight force by a flapping wing: lift and drag production. J Exp Biol 2001;204:2607.
19. Usherwood JR, Ellington CP. The aerodynamics of revolving wings II. Propeller force coefficients from mayfly to quail. J Exp Biol 2002;205:1565.
20. Fry SN, Sayaman R, Dickinson MH. The aerodynamics of free-flight maneuvers in Drosophila. Science 2003;300:495.
21. Fry SN, Sayaman R, Dickinson MH. The aerodynamics of hovering flight in Drosophila. J Exp Biol 2005;208:2303.
22. Altshuler DL, Dickson WB, Vance JT, Roberts SP, Dickinson MH. Shortamplitude high-frequency wing strokes determine the aerodynamics of honeybee flight. PNAS 2005;102:18213.
23. Liu H, Ellington CP, Kawachi K, van den Berg C, Willmott AP. A computational fluid dynamic study of hawkmoth hovering. J Exp Biol 1998;201:461.
24. Wang ZJ. Two dimensional mechanism for insect hovering. Phys Rev Lett 2000;85:2216.
25. Sun M, Tang J. Unsteady aerodynamic force generation by a model fruitfly wing in flapping motion. J Exp Biol 2002;205:55.
26. Wu JH, Sun M. Unsteady aerodynamic forces of a flapping wing. J Exp Biol 2004;207:1137.
27. Sun M, Lan SL. A computational study of the aerodynamic forces and power requirements of dragonfly (Aeschna juncea) hovering. J Exp Biol 2004;207:1887.
28. Wang ZJ. The role of drag in insect hovering. J Exp Biol 2004;207:4147.
29. Wang ZJ, Russell D. Effect of forewing and hindwing interactions on aerodynamic forces and power in hovering dragonfly flight. Phys Rev Lett 2008;99:148101.
30. Bos FM, Lentink D, Oudheusden BWV, Bijl H. Influence of wing kinematics on the aerodynamic performance in hovering insect flight. J Fluid Mech 2008;594:341.
31. Muijres FT, Johansson LC, Barfield R, Wolf M, Spedding GR, Hedenström A. Leading-edge vortex improves lift in slow-flying bats. Science 2008;319:1250.